JCB Article

Minus-end capture of preformed kinetochore fibers contributes to spindle morphogenesis

Alexey Khodjakov,[1,2] Lily Copenagle,[4] Michael B. Gordon,[3] Duane A. Compton,[3] and Tarun M. Kapoor[2,4]

[1]Division of Molecular Medicine, Wadsworth Center, New York State Department of Health, Albany, NY 12201
[2]Marine Biology Laboratory, Woods Hole, MA 02543
[3]Department of Biochemistry, Dartmouth Medical School, Hanover, NH 03755
[4]Laboratory of Chemistry and Cell Biology, The Rockefeller University, New York, NY 10021

Near-simultaneous three-dimensional fluorescence/differential interference contrast microscopy was used to follow the behavior of microtubules and chromosomes in living α-tubulin/GFP-expressing cells after inhibition of the mitotic kinesin Eg5 with monastrol. Kinetochore fibers (K-fibers) were frequently observed forming in association with chromosomes both during monastrol treatment and after monastrol removal. Surprisingly, these K-fibers were oriented away from, and not directly connected to, centrosomes and incorporated into the spindle by the sliding of their distal ends toward centrosomes via a NuMA-dependent mechanism. Similar preformed K-fibers were also observed during spindle formation in untreated cells. In addition, upon monastrol removal, centrosomes established a transient chromosome-free bipolar array whose orientation specified the axis along which chromosomes segregated. We propose that the capture and incorporation of preformed K-fibers complements the microtubule plus-end capture mechanism and contributes to spindle formation in vertebrates.

Introduction

For accurate segregation of replicated genetic material into two daughter cells, sister kinetochores on each chromosome must establish stable connections with the opposite poles of the spindle. Kirschner and Mitchison (1986) proposed a model that provides powerful explanations for how spindle formation occurs in vertebrate somatic cells. In this model, centrosomes nucleate a radial array of dynamic microtubules whose plus ends are captured and selectively stabilized by kinetochores. Over time, these initial microtubule attachments mature to form kinetochore fibers (K-fibers).* Several lines of evidence, including direct observations of microtubule capture by kinetochores (Rieder and Alexander, 1990), have provided extensive experimental support for this hypothesis (for review see Rieder and Salmon, 1998).

In its original form, the plus-end search and capture model implies that all kinetochore microtubules are derived from astral microtubules nucleated from centrosomes. However, spindle assembly has been shown to occur efficiently in the absence of centrosomes in extracts prepared from frog eggs through a mechanism that relies on microtubule nucleation and organization in the vicinity of chromosomes (Heald et al., 1996; Walczak et al., 1998; for review see Karsenti and Vernos, 2001). Recent studies reveal that this chromosome-directed mechanism for spindle assembly is operative in cell types that normally form a typical "astral" spindle, as eliminating centrosome activity by laser micro-ablation (Khodjakov et al., 2000) or genetic mutations (Bonaccorsi et al., 1998; Megraw et al., 2001) did not prevent formation of functional bipolar spindles. Moreover, recent experiments suggest that proteins acting downstream of Aurora A kinase and Ran GTPase to promote chromosome-directed spindle organization in frog egg extracts may be playing similar roles in vertebrate somatic cells (Gruss et al., 2002; Kufer et al., 2002); however, direct evidence for this is currently limited. These observations indicate that mechanisms other than plus-end search and capture contribute to spindle assembly in vertebrate cells and cast doubt that all K-fibers arise from captured astral microtubules.

One of the problems in determining whether K-fibers can form by mechanisms not involving centrosomes is that in bipolar spindles, chromosomes typically have each of their two kinetochores oriented toward one of the two separated centrosomes. Under these conditions, forming K-fibers become

The online version of this article includes supplemental material.

Address correspondence to Tarun M. Kapoor, 1230 York Ave., The Rockefeller University, New York, NY 10021. Tel.: (212) 327-8176. Fax: (212) 327-8177. E-mail: kapoor@rockefeller.edu

*Abbreviations used in this paper: 2- and 3-D; two and three dimensional; DIC, differential interference contrast; K-fiber; kinetochore fiber; NEB, nuclear envelope breakdown.

Key words: mitosis; mitotic spindle; microtubules; spindle pole; chromosome positioning

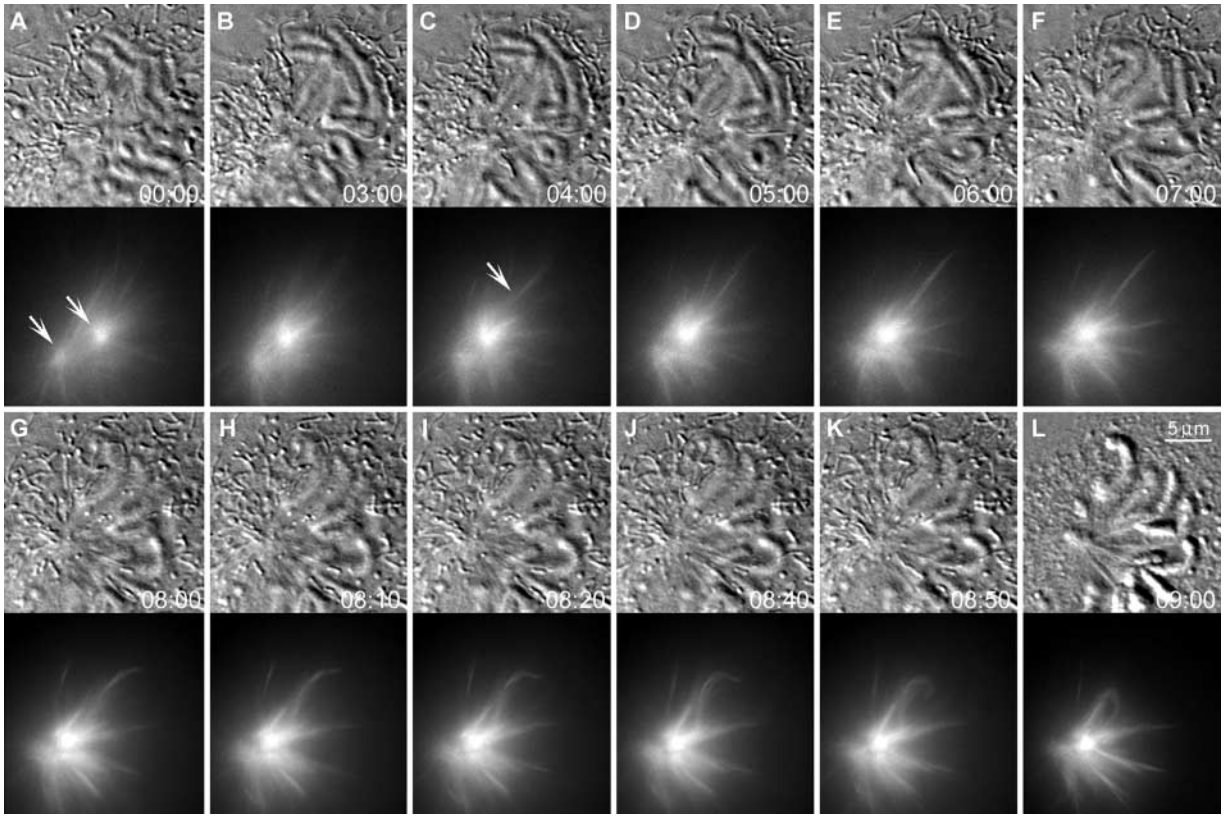

Figure 1. **Formation, looping, and incorporation of microtubule bundles in monastrol-induced monopolar spindles in PtK-αT cells.** Selected frames are shown from a near-simultaneous 3-D fluorescence/DIC time-lapse microscopy experiment. The top half of each image represents a DIC slice through the central part of the cell, whereas the bottom half is a maximal intensity projection of a 3-D fluorescence volume recorded at 0.5-μm Z-steps. After NEB, both centrosomes come together (A, arrows) and form a common pole. The chromosomes orient toward the unseparated centrosomes and surround the pole (B and C). A new microtubule bundle (C, arrow), not associated with the centrosomes, forms and rapidly grows outwards (compare C–E), reaching 10-μm length in 3 min (E). This bundle begins to bend (G) and its distal tip moves toward the pole (H–J). As a result, the bundle forms a loop with both ends embedded into the central part of the spindle (K). At this point, the cell was fixed and permeabilized for immunofluorescence analysis (L; see also Fig. 2). Video 1 (available at http://www.jcb.org/cgi/content/full/jcb.200208143/DC1) shows similar microtubule dynamics in another monastrol-treated PtK-αT cell. Time is in minutes:seconds.

submerged in a mass of astral and interpolar microtubules that obscure direct visualization of individual K-fiber behavior. This limitation can be overcome by following the behavior of microtubules associated with the kinetochores distal to centrosomes in monopolar spindles.

Formation of monopolar spindles in vertebrates occurs when the centrosomes fail to separate before nuclear envelope breakdown (NEB; Roos, 1976; Cassimeris et al., 1994) or when they separate too far from one another (anaphase-like prometaphase; Bajer, 1982; Rieder and Hard, 1990). In both cases, the monopolar configurations are transient, and over time, these structures transform into functional bipolar spindles as centrosomes separate or come closer together (in the case of anaphase-like prometaphase). Although naturally occurring monopolar spindles have proven to be a valuable model for studying mechanisms of mitosis, their rarity and the unpredictable time before they transform into bipolar arrays limit their usefulness. Monastrol, a small molecule inhibitor of the mitotic kinesin Eg5, provides a convenient tool by which monopolar spindles can be induced (Mayer et al., 1999; Kapoor et al., 2000). Unlike other known small molecule inhibitors of mitotic proteins, monastrol does not perturb microtubule dynamics (Mayer et al., 1999). Thus, monastrol-induced monopolar spindles present a unique opportunity to examine the behavior of K-fibers in vertebrate mitoses. Further, the rapid reversibility of the monastrol arrest allows precise temporal control over the transition of monopolar arrays to bipolar spindles. Combining the use of monastrol and high-resolution multidimensional microscopy, we have obtained direct evidence for a mechanism other than plus-end search and capture that contributes to spindle morphogenesis in vertebrate cells. Our data also reveal how centrosomes contribute to the organization of bipolar spindles before chromosome segregation.

Results

Capture and incorporation of preformed microtubule bundles into the monopolar spindle in monastrol-treated cells

We used near-simultaneous three-dimensional (3-D) GFP fluorescence/two-dimensional (2-D) differential interference contrast (DIC) multimode microscopy to follow the behavior of both the microtubules and chromosomes in live monastrol-treated PtK_2 cells that express α-tubulin/GFP (PtK-

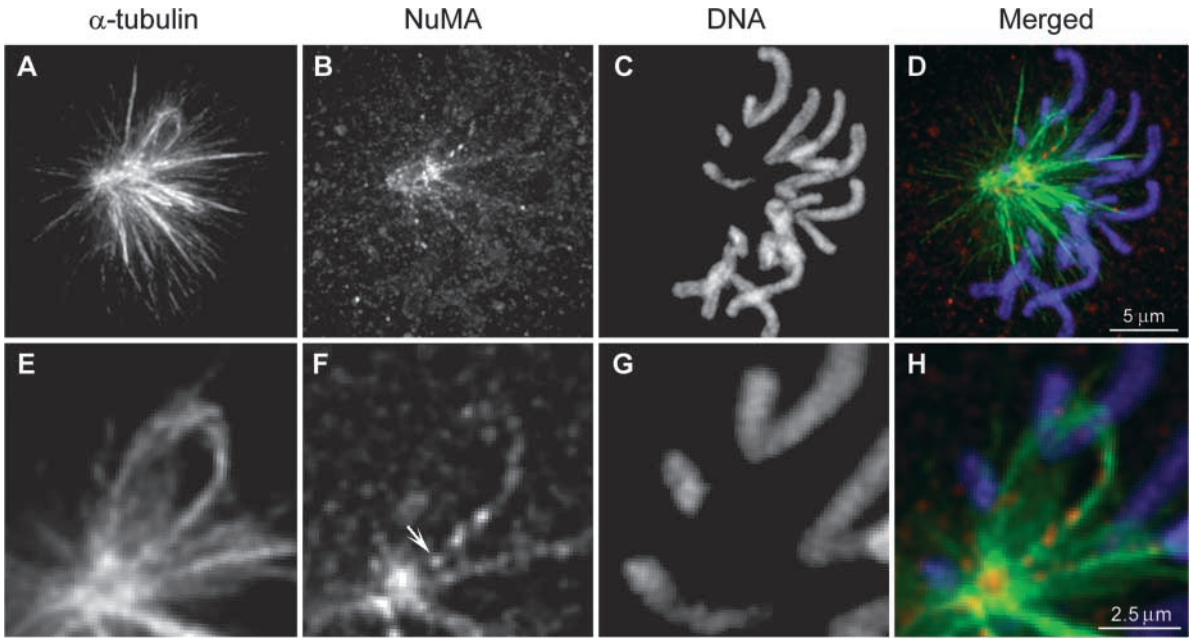

Figure 2. **Small aggregates of NuMA are associated with the parts of the microtubule loop that move poleward.** Same cell as in Fig. 1. (A–D) Maximal projections of 3-D fluorescence volumes representing microtubules (anti–α-tubulin; A), NuMA (rabbit polyclonal; B), chromosomes (Hoechst 33342; C), and a pseudocolored overlay of these three channels (D). (E–H) Individual slices of the 3-D volumes presented in A–D, at higher magnification. Note that NuMA is present along the microtubule bundles that extend toward the periphery of the spindle and on the leading half of the loop (B and F, arrow).

αT). Typically, we began observation immediately after NEB and then followed the cell for 2 h, recording one DIC image and a corresponding 3-D fluorescence stack every minute. In some experiments (e.g., Fig. 1), we followed cells over shorter periods (10–30 min) but at higher temporal resolution (10–30-s intervals).

Our 2-h time-lapse recordings of 20 cells revealed that within 5–10 min after NEB, all chromosomes in monastrol-treated cells became mono-oriented and assumed a star-like configuration, with their centromere regions oriented toward the centrosomes and the arms pointing outwards (see Video 1, available at http://www.jcb.org/cgi/content/full/jcb.200208143/DC1). At the moment of NEB in the presence of monastrol, the centrosomes were often already spatially separated (Fig. 1). This has also been observed in untreated PtK cells (Roos, 1976). In the presence of monastrol, centrosomes generated two radial microtubule arrays that coalesce within a few minutes after NEB (Fig. 1). Initially, the chromosomes may be positioned only on one side of the centrosomes, but, over time, they gradually rearranged into a spherical array encircling the centrosomes. These aspects of monopolar spindle formation were largely expected from previous fixed cell analyses of monastrol-treated cultures (Mayer et al., 1999, Kapoor et al., 2000).

One unexpected feature conspicuous in our time-lapse recordings was that in all cells imaged, we observed prominent bundles of microtubules extending from the chromosomes toward the cell periphery. These bundles appeared in the vicinity of the centromere regions of chromosomes and then rapidly grew outwards (Fig. 1). Temporal resolution in most of our time-lapse records was not sufficient to determine precise elongation rates of the bundles that can often reach up to 10–12 μm within 3 min. To document these events in greater detail, we used a spinning-disk confocal microscope, which acquired images at a higher temporal resolution, sampling the cellular volume every 15 s. Under these conditions, we observed elongation rates of ~3–4 μm/min (see Fig. S1, available at http://www.jcb.org/cgi/content/full/jcb.200208143/DC1).

After reaching ~10 μm in length, the bundles usually underwent a rapid bending, and their ends distal to the chromosome moved back toward the center of the spindle (Fig. 1). As a result, the bundle formed a transient microtubule "loop" as its distal end moved inwards to the pole while the proximal end remained relatively stationary. This configuration was transient, and in ~2–5 min, the bundle made a complete 180° turn so that its distal end incorporated into the spindle. Overall, this behavior is suggestive of the distal end of the microtubule bundle being suddenly captured and experiencing a force directed toward the center of the spindle.

The phenomenon of formation, capture, and incorporation of microtubule bundles was very common in monastrol-induced monopolar mitoses. On average, we observed ~10–12 such events in a cell during a 2-h observation period (range 8–20; 19 events in Video 1). Once a bundle of microtubules formed (reached ~10-μm length), it was typically captured within 5 min. Infrequently, some bundles remained extended for up to 15–20 min before incorporating into spindles.

This microtubule formation, capture, and incorporation phenomenon is not limited to the PtK-αT cells. We also observed similar behavior of microtubule bundles in other cell types, including LLC-PK and CV-1 (both constitutively expressing α-tubulin/GFP; unpublished data).

Microtubule loops result in the formation of syntelic-oriented chromosomes in monastrol-treated cells

To determine the structural organization of microtubule loops, we followed a cell by 3-D fluorescence/ 2-D DIC microscopy and then fixed it during a microtubule looping event. The fixed cells were subsequently processed for immunofluorescence analysis. This analysis revealed that the proximal end of the microtubule bundle (one that remains stationary during looping) was always associated with the primary constriction of a chromosome (Fig. 2). As a result, upon incorporation of the distal end of the looping microtubule bundle into the spindle, the chromosome becomes syntelic, i.e., its primary constriction connected to the spindle pole by two bundles of microtubules (Fig. 2). This configuration implies that before the distal microtubule bundle was captured and looped toward the spindle pole, it extended from the primary constriction toward the cell periphery. To confirm this, we analyzed a population of monastrol (100 μM)-induced monopolar mitoses in PtK-αT cells after fixation and immunostaining for microtubules, kinetochores, and chromosomes. Our analysis revealed that ~10% of monopolar mitoses contain conspicuous bundles of microtubules that emanate directly from distal kinetochores and extend for several micrometers away from the spindle pole and toward the cell's periphery (Fig. 3, A–D).

To investigate the structural organization of these distal K-fibers at a greater resolution, we analyzed two monopolar mitoses in a population of PtK cells treated with 100 μM

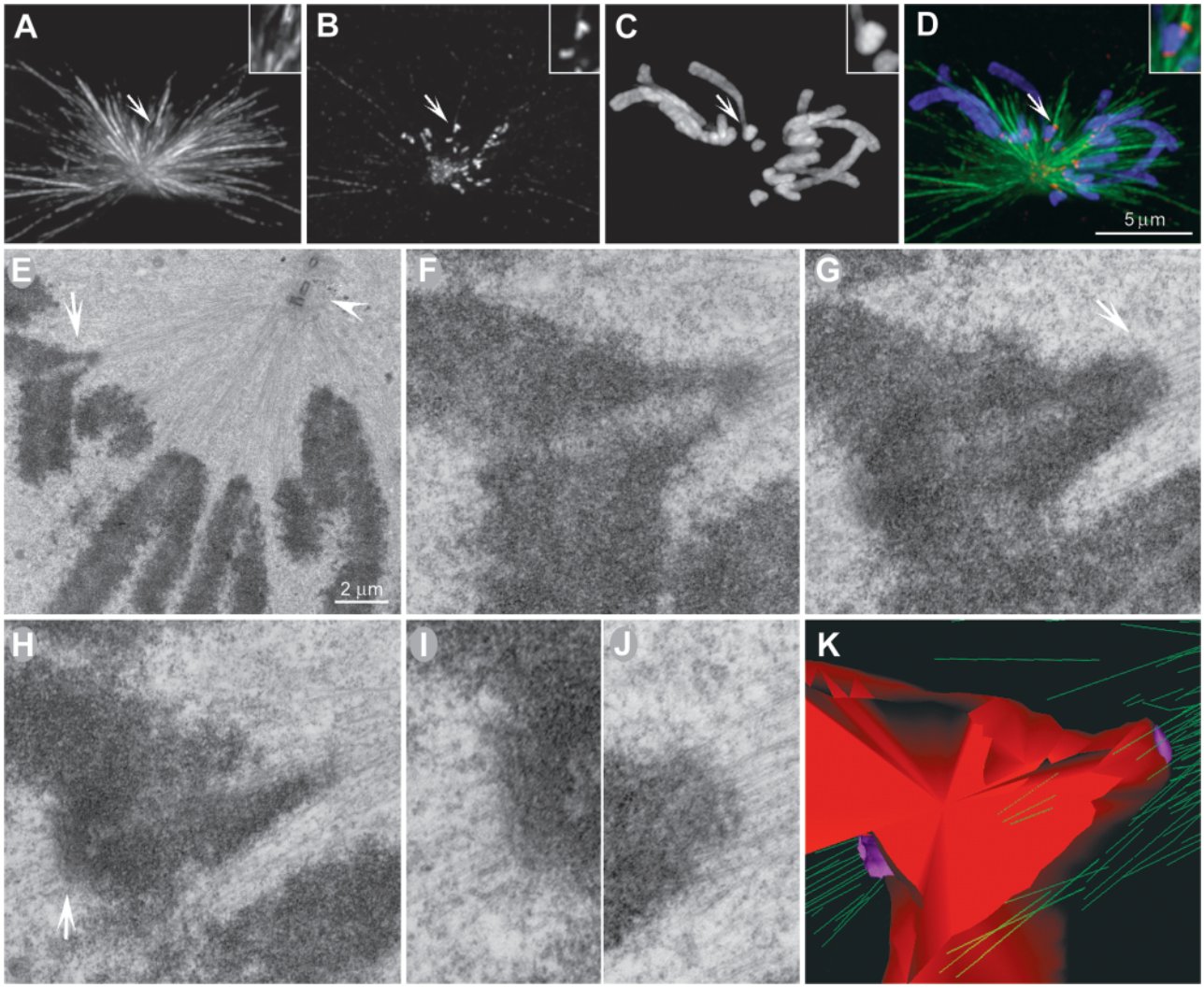

Figure 3. **Some of the distal kinetochores in monastrol-induced monopolar spindles are associated with well-developed bundles of microtubules (K-fibers).** (A–D) A PtK-αT cell stained for microtubules (anti-α-tubulin; A), kinetochores (anti-CENP-E; B), and chromosomes (Hoechst 33342; C). Note a prominent bundle of microtubules (A, arrow) emanating from the distal kinetochore (B, arrow) of one of the mono-oriented chromosomes (C, arrow) and extending toward the cell's periphery. (D) A composite of all three channels. Insets in each panel are at 2×. (E–K) A PtK-αT cell analyzed by serial section EM. (E) Lower magnification overview of the cell. Both centrosomes remain unseparated (three centrioles are present within this section [E, arrowhead] and the fourth one is in the adjacent section). (F and G) Serial 0.25-μm sections through the primary constriction of one of the chromosomes (E, G, and H, arrows). Well-developed bundles of microtubules emanate from both the proximal (G) and the distal (H) kinetochores. (I and J) Higher magnification of G and H. (K) Surface-rendered model based on serial section reconstruction of the chromosome presented in F–H. Note that both the proximal and the distal kinetochores are associated with similar numbers of microtubules.

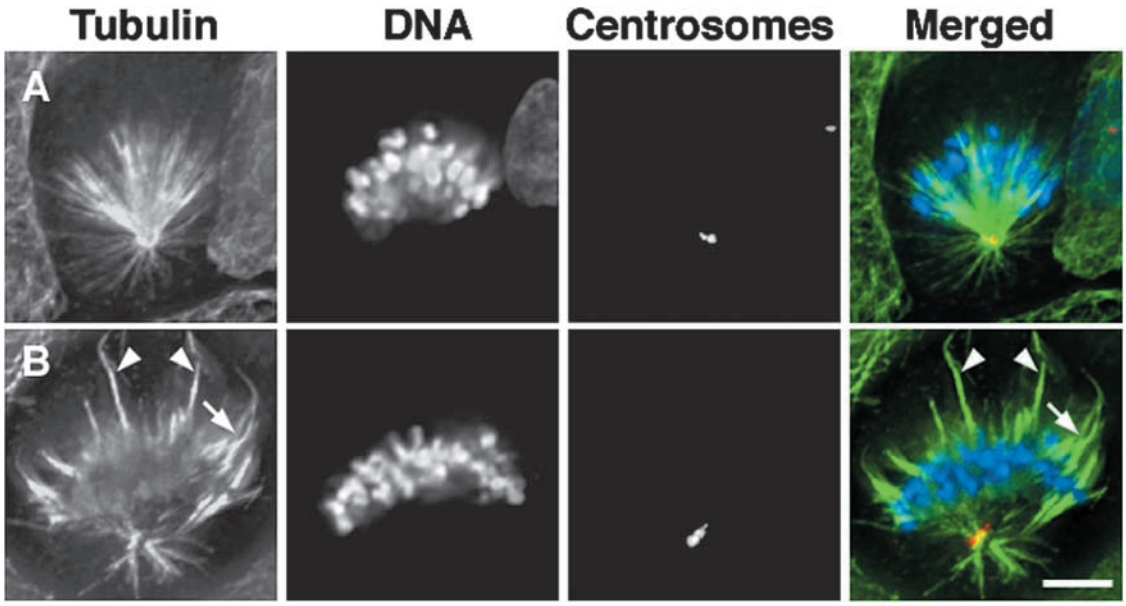

Figure 4. **NuMA is required for K-fiber orientation in monopolar spindles formed in cells lacking Eg5 activity.** Human CFPAC-1 cells treated with 100 μM monastrol (A) or injected with both Eg5- and NuMA-specific antibodies (B) were fixed in mitosis. Mitotic spindle morphology was visualized in these cells by staining for microtubules using the tubulin-specific monoclonal antibody DM1α, for centrosomes using a human centrosome-specific autoimmune serum, and for DNA using DAPI. Arrowheads highlight K-fibers, and the arrow points to a group of K-fibers that appear to be focused into a small spindle pole. Bar, 20 μm.

monastrol by serial section EM. The cells were selected without bias, and spindle structures were not evaluated by immunofluorescence before processing for EM. Nevertheless, in these two cells, we found three unambiguous cases of well-developed K-fibers emanating from distal kinetochores toward the cell periphery (Fig. 3, E–K). Each individual kinetochore plate was associated with several microtubules (up to 12). It is important to emphasize that in all three cases, the distal kinetochore faced directly away from the spindle pole and was shielded from the astral microtubules by the chromosome mass (Fig. 3, E–K). Thus, our serial section EM data confirmed the existence of K-fibers not directly oriented to the spindle pole.

Inhibition of NuMA prevents microtubule fiber looping

Thus far, our data revealed that microtubule loops form when the free ends of preformed K-fibers are captured and actively transported toward the spindle pole. To examine the molecular mechanism of this poleward sliding of spindle microtubules, we examined the localization of NuMA, a protein responsible for maintaining microtubule ends focused at spindle poles (Gaglio et al., 1995; Merdes et al., 1996; Gordon et al., 2001). We found NuMA to be present at the leading end of the looping microtubule bundle in all cells analyzed ($n = 4$) (Fig. 2 F, arrow). Because NuMA has been shown to interact with the dynein/dynactin complex (Merdes et al., 1996), this observation is consistent with the capture and incorporation of microtubule bundles being driven by dynein motility.

To test whether NuMA activity is required for microtubule looping, we microinjected cells with a NuMA-specific antibody (Gaglio et al., 1996). We previously demonstrated that injection of this antibody into cultured cells aggregates NuMA and prevents it from interacting appropriately with spindle microtubules (Gaglio et al., 1996; Gordon et al., 2001). For these experiments, we used human CFPAC-1 cells, as available anti-NuMA antibodies do not react sufficiently with marsupial NuMA to inhibit its function in PtK cells. Inhibition of Eg5 function in human CFPAC-1 cells through either injection of Eg5-specific antibodies (unpublished data) or monastrol treatment prevented centrosome separation and led to the formation of monopolar spindles (Fig. 4 A). The microtubule distribution in these monopolar spindles was indistinguishable from that observed in PtK-αT cells, with only a few microtubule bundles extending toward the cell periphery (on average one bundle in every other cell; data from 16 cells analyzed by 3-D microscopy). In contrast, upon simultaneous perturbation of Eg5 (by either treatment with monastrol [unpublished data] or injection of Eg5-specific antibodies) and NuMA (by antibody injection), numerous straight microtubule bundles were seen to extend from the chromosomes in an orientation opposite that of the pole defined by the two unseparated centrosomes (Fig. 4 B; on average five to six bundles per cell; data from 17 cells analyzed by 3-D microscopy). If monastrol was removed from cells injected with NuMA antibodies and treated with monastrol, then we observed centrosome separation, but K-fibers failed to recruit appropriately toward the centrosomes (unpublished data), resulting in disorganized spindles with splayed spindle poles analogous to those observed after perturbation of NuMA alone (Gaglio et al., 1996; Gordon et al., 2001). These changes in microtubule distribution are consistent with the idea that NuMA is functionally responsible for the capture and incorporation of preformed K-fibers. Upon inhibition of NuMA, the fibers that would normally loop back to the single pole remained extended and accumulated over time.

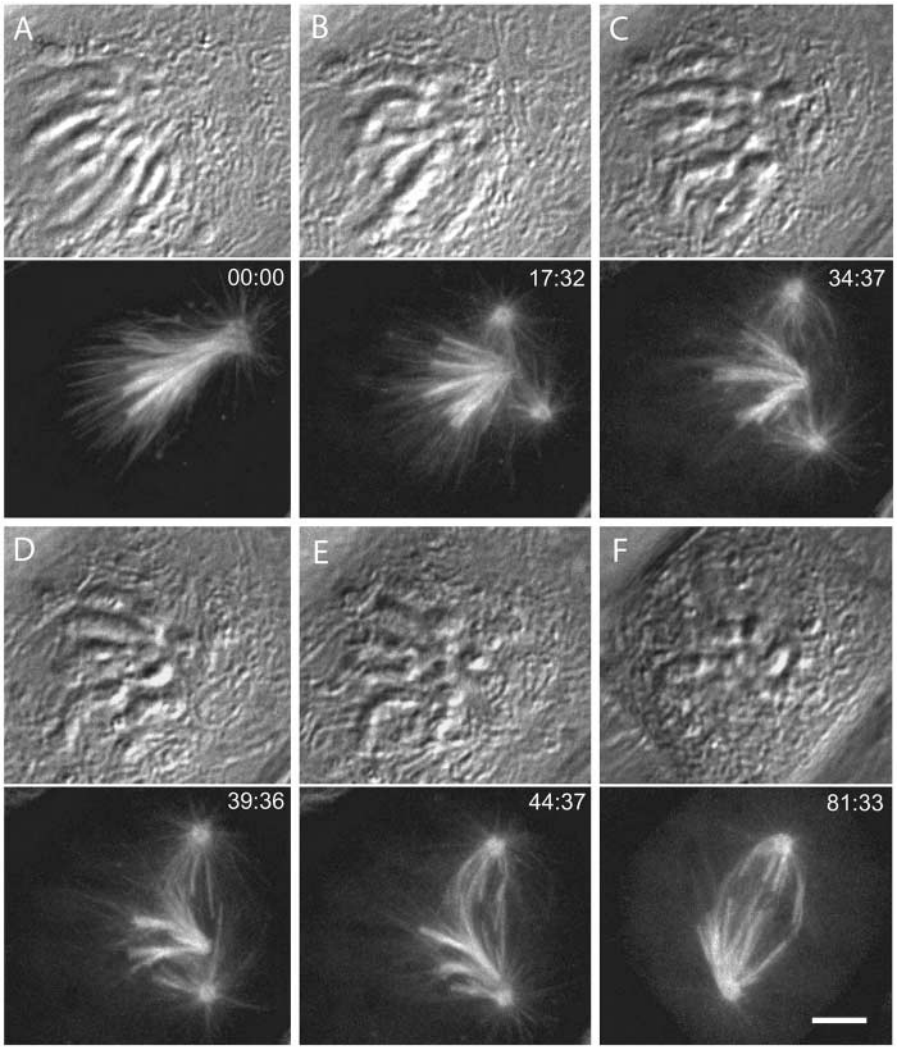

Figure 5. **The "capture" of stable K-fiber minus ends contributes to bipolar spindle formation and chromosome alignment in PtKαT cells released from a monastrol arrest.** Selected frames from a near-simultaneous 3-D confocal fluorescence/2-D DIC time-lapse microscopy experiment are shown. At each time point, a DIC image from a focal plane in the center of the cell is presented with the maximum intensity projection of confocal fluorescence sections of a 6-μm-thick Z-series acquired in 1.5-μm steps. (A) A monopolar spindle within 60 s after removal of monastrol from the cell medium. (B) At early time points, a small bipolar array of microtubules forms at the center of the mono-aster. (C) Several K-fibers maintain their astral arrangement while the bipolar array increases in length and establishes the dominant spindle axis. K-fibers not associated with the poles of the emerging bipolar spindle support robust chromosome oscillations (see Videos 2A and 2B, available at http://www.jcb.org/cgi/content/full/jcb.200208143/DC1). (D–F) Stable minus ends of these K-fibers are eventually drawn toward the poles of the bipolar microtubule array and chromosomes align. Time is shown in minutes:seconds. Bar, 5 μm.

Capture of preformed microtubule bundles occurs during spindle bipolarization after monastrol washout

The mitotic arrest due to monastrol is completely reversible, and monopolar spindles rapidly rearrange into normal bipolar mitoses upon monastrol washout (Kapoor et al., 2000). To investigate whether the capture and looping of preformed microtubule bundles occurs during the transformation of monopolar structures into bipolar spindles, we examined microtubule behavior in cells released from monastrol arrest. Our initial attempts to follow these transformations revealed that the redistribution of microtubules can often be too complex to be followed by wide-field fluorescence microscopy. Therefore, we employed near-simultaneous 3-D confocal fluorescence/2-D DIC time-lapse microscopy for these experiments. The use of a spinning-disk confocal microscope allowed us to track individual microtubule bundles within complex arrays with greater precision than conventional wide-field fluorescence microscopy. Scanning depth was set to match the parameters of our wide-field time-lapse recordings used to examine cells in the presence of monastrol. Images sampling the cell volume were acquired at 30-s intervals.

Our recordings revealed that bipolarization of the spindle began immediately upon monastrol removal, and cells consistently initiated anaphase ~75 min after washout. The bipolarization began with the separation of centrosomes, which often detached from the rest of the spindle (Figs. 5 and 6). Intriguingly, the orientation of the axis of centrosome separation was not related to the original orientation of the K-fibers within the monopolar spindle, and the centrosomes often separated in a direction perpendicular to the majority of the K-fibers (Fig. 5). As the centrosomes separated, they remained associated with prominent arrays of astral microtubules. These microtubules overlap and appear to interact, forming a structure very similar to the "chromosome-free spindles" described by Faruki et al. (2002) in PtKαT polykaryons. Detachment of centrosomes did not immediately affect the organization of the monopolar spindle. K-fibers remained focused at a single spindle pole that now lacked astral microtubules (Fig. 5 B). These K-fibers exhibited rapid changes in length corresponding to oscillations of attached chromosomes (see Videos 2 and 3, available at http://www.jcb.org/cgi/content/full/jcb.200208143/DC1).

Importantly, during bipolarization of the spindle, the K-fibers continued to exhibit capture and incorporation of their minus ends into the spindle. However, in contrast to monopolar spindles where K-fibers looped around chromosomes and became incorporated into the single spindle pole, during bipolarization of the spindle, each bundle exhibited

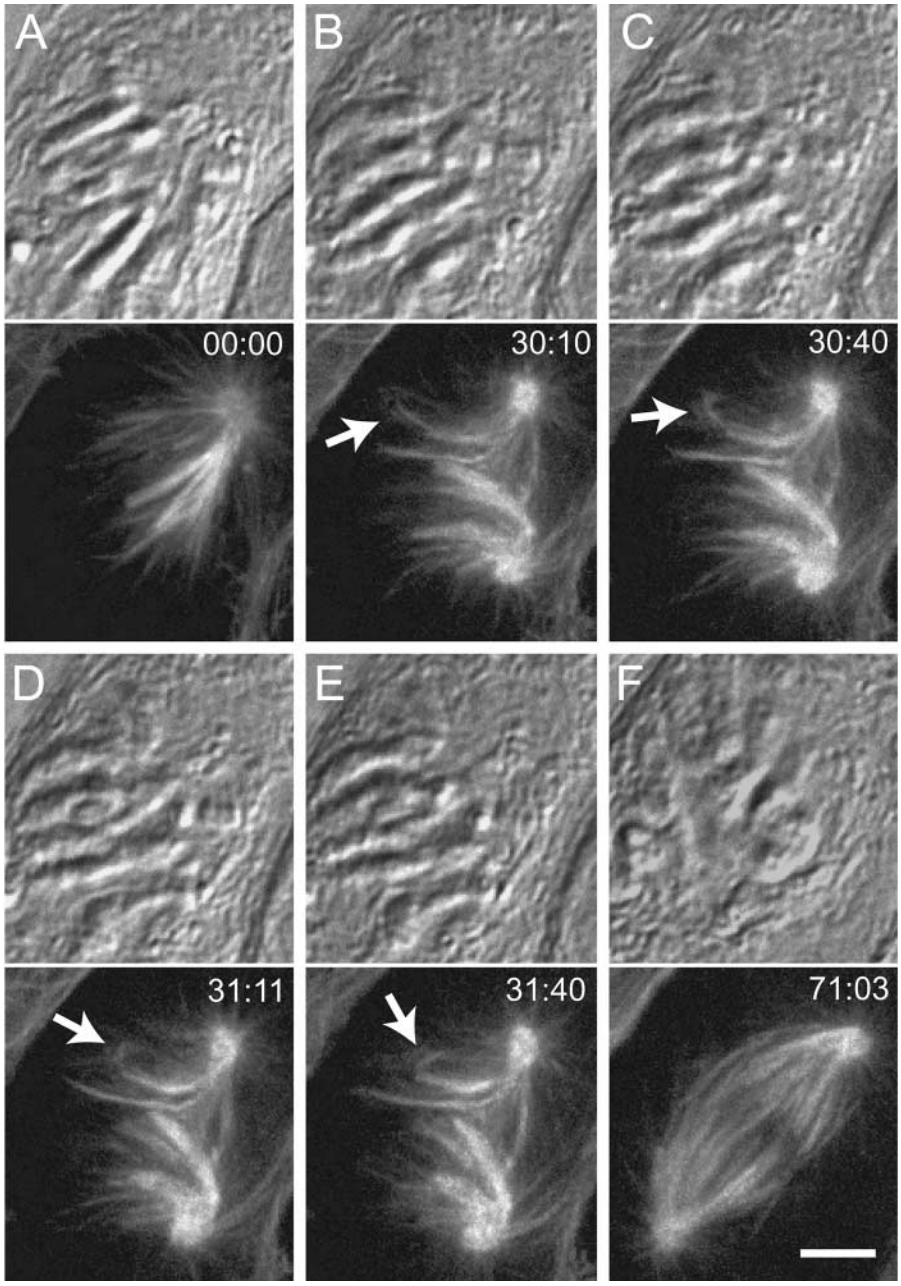

Figure 6. **Looping and capture of microtubules contributes to spindle morphogenesis in PtKαT cells released from a monastrol arrest.** PtKαT cells with monopolar spindles formed in the presence of 100 μM monastrol were placed in monastrol-free medium, and the first image (time = 0:00) of the near-simultaneous 3-D confocal fluorescence/DIC time-lapse microscopy experiment was acquired within 60 s. Each time point shows a DIC image from a focal plane in the center of the cell (above) and a maximum intensity projection of confocal fluorescence Z-sections of a 6-μm-thick Z-series acquired at 1.5-μm steps (below). (A) Microtubules in a mono-astral array are shown in a PtKαT cell immediately after the removal of monastrol. (B–E) The formation and looping of a microtubule bundle from the distal end of an existing K-fiber (arrow) is shown. This microtubule bundle is captured (E) to form a connection to the spindle pole proximal to the minus end of the microtubule bundle from which this fiber emerged (see Videos 3A and 3B, available at http://www.jcb.org/cgi/content/full/jcb.200208143/DC1). Time is shown in minutes:seconds. Bar, 5 μm.

one of two types of motion. First, those K-fibers that emanated from the side of chromosomes that faced the centrosomes exhibited direct translocations toward one of the two separating centrosomes. As a result, each chromosome became either syntelic (when minus ends of both K-fibers were captured by the same centrosome) or properly bioriented (Fig. 5). Second, those K-fibers that emanated from chromosomes toward the cell's periphery behaved exactly as the distal K-fibers in monopolar spindles. The K-fibers bended and looped around chromosomes, with their minus ends sliding toward one of the two separating centrosomes (Fig. 6).

Capture and incorporation of K-fiber minus ends was a common phenomenon we observed in every cell released from a monastrol arrest. Looping of K-fibers distal to the centrosome was often seen during the initial stages of spindle bipolarization with an average frequency of seven loops per cell (range 1–24; $n = 15$). The high density of microtubules on the side proximal to the centrosomes precluded accurate quantification of direct translocations of K-fiber minus ends toward the separated centrosomes. However, this phenomenon was at least as common as the "looping" of distal K-fibers during the initial stages of spindle bipolarization and predominant during later stages (Videos 2 and 3).

Our observations reveal that spindle morphogenesis in vertebrates does not only depend on the microtubule plus-end search and capture mechanism but also includes the capture and incorporation of preformed K-fibers at their minus ends.

NuMA is consistently associated with the minus ends of K-fibers during spindle bipolarization

Our data have shown that minus ends of distal K-fibers incorporating into monopolar spindles were always associated

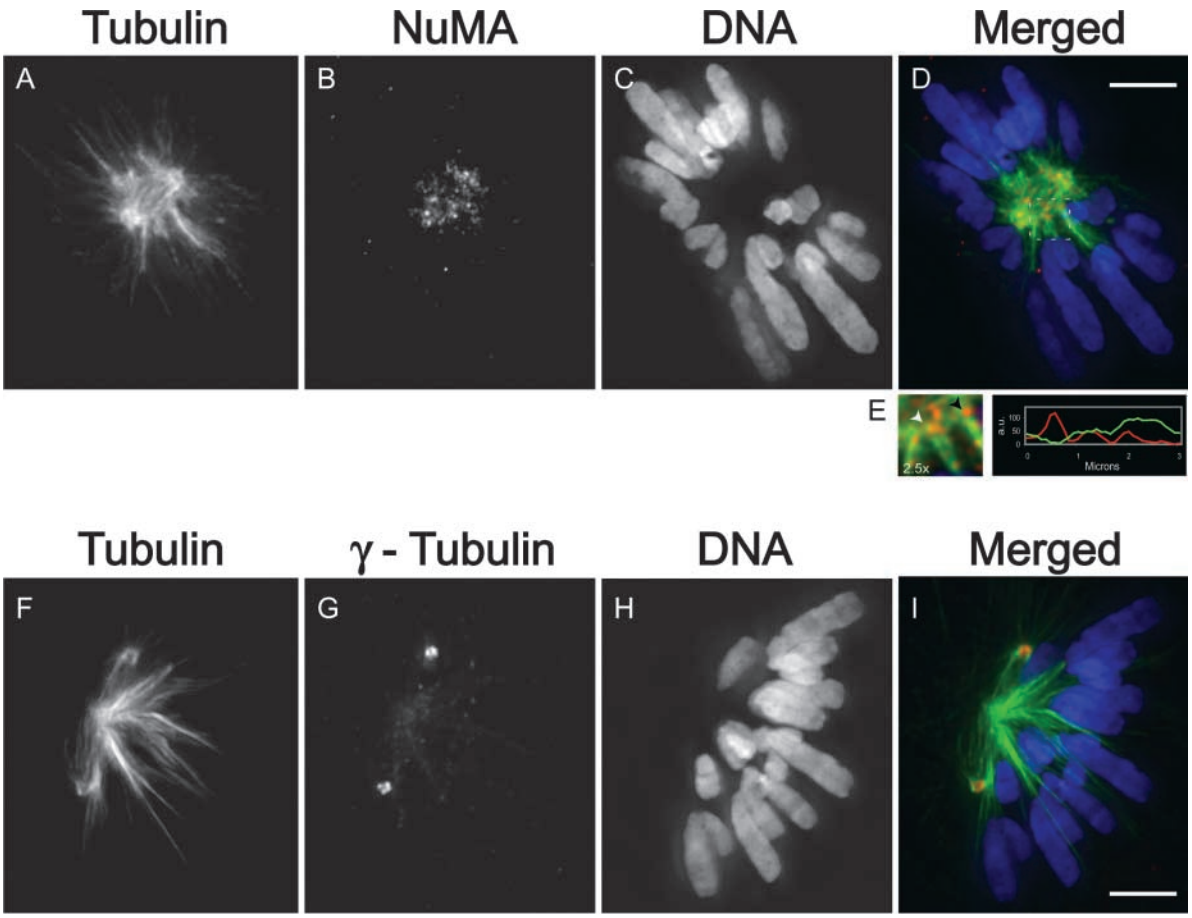

Figure 7. **In cells establishing bipolar spindles after release from a monastrol arrest, kinetochore microtubule minus ends are associated with interpolar microtubules and NuMA but not centrosomes.** (A–D) PtK2 cells arrested in the presence of monastrol (100 μM) for 3 h were transferred to monastrol-free media and fixed after 26 min. The distribution of α-tubulin (A), NuMA (B), and DNA (C) in a cell is shown. (E) An enlarged view shows NuMA localized to discrete points along the spindle, which are brightest at the intersections of kinetochore microtubule minus ends and microtubules (arrowheads) in an emerging bipolar array. A line scan along the K-fiber indicated by the black arrowhead compares NuMA and tubulin distribution (NuMA, red; tubulin, green). (F–I) In an independent experiment, a PtK2 cell released from a monastrol arrest was fixed after 10 min and processed for immunofluorescence. The organization of α-tubulin (F), γ-tubulin (G), and DNA (H) in the cell is shown. Note that γ-tubulin is concentrated at the spindle poles separated by an interpolar network of microtubules. Intersections between kinetochore microtubule bundles and the interpolar microtubules are observed at almost right angles. Three-color overlays are shown in D and I. Images are maximum intensity projections of deconvolved fluorescence image volumes. Bars, 5 μm.

with NuMA (see above). To determine if this was the case for the persistent K-fibers that faced centrosomes and exhibited more direct translocation toward a centrosome, we examined the distribution of NuMA in cells released from a monastrol arrest (Fig. 7, A–E). In all cells examined, NuMA was distributed in numerous small patches spread over the region between the separating centrosomes. The strongest NuMA staining corresponded to the ends of K-fibers (Fig. 7 E; 2.5× magnification of three-color overlay and line scan). This is consistent with our data that NuMA function is required for the capture and incorporation of the preformed K-fibers into the mitotic spindle.

The fact that NuMA was consistently spread over a large area between the separating centrosomes raised a formal possibility that centrosomal material was similarly fragmented in cells released from monastrol. To evaluate this, we examined localization of γ-tubulin, a protein that has been shown to delineate the boundaries of centrosomes (Khodjakov and Rieder, 1999). This analysis revealed that in contrast to the NuMA distribution, the centrosomal material remained focused at the spindle poles, and thus the centrosomes were not fragmented under these conditions (Fig. 7, F–I). Overall, these observations suggest that common mechanisms contribute to the capture and incorporation of K-fiber minus ends in monopolar spindles and during spindle bipolarization.

Capture of preformed microtubule bundles occurs during mitotic spindle formation in control cells

Thus far, our data revealed that capture and incorporation of preformed K-fibers contributes to spindle morphogenesis in cells treated with monastrol. The question remained whether this phenomenon also occurs during normal bipolar spindle formation in unperturbed cells. We reviewed a library of time-lapse recordings of spindle formation in control PtK-αT cells (~20 cells) and found two examples of clear incorporation of preformed K-fibers into the forming spindle. Fig. 8 illustrates one such event (see Video 4, available at http://www.jcb.org/cgi/content/full/

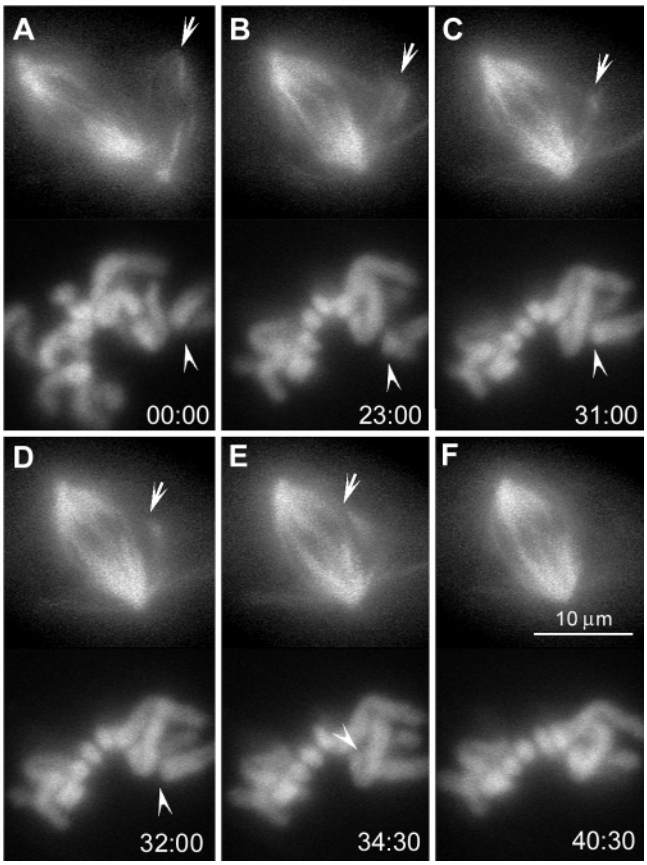

Figure 8. **Capture and incorporation of preformed K-fibers into the spindle occurs during spindle formation in control PtK cells.** Selected frames from a fluorescence time-lapse recording of a PtK-αT cell also stained with Hoechst 33342 to visualize chromosomes. The top half of each image represents the green channel (α-tubulin/GFP), and the bottom half represents the blue (Hoechst 33342) channel. Arrows in A–E point at a bundle of microtubules that initially forms in association with one of the chromosomes (A–E, arrowheads). This bundle persists for ~30 min until it begins to slide toward the distal spindle pole (D–E) and eventually incorporates into the spindle (F) (see Video 4, available at http://www.jcb.org/cgi/content/full/jcb.200208143/DC1). Time is in minutes:seconds.

jcb.200208143/DC1. In both cases, the fibers were incorporated into the correct half spindle, resulting in accurate biorientation of the chromosome.

Discussion

Three key insights into the morphogenesis of the mitotic spindle

Kinetochore microtubule fibers can form without direct connections to centrosomes. We consistently observed prominent microtubule bundles that were not connected to the centrosomes but emanated from primary constrictions of chromosomes (kinetochores). Serial section EM analysis of monopolar mitoses confirmed the existence of well-developed bundles of parallel microtubules that terminated within trilaminar plates of distal kinetochores. These bundles were seen to extend from kinetochores that were often completely shielded from the centrosomes by chromosome masses surrounding the kinetochore. Such a configuration excluded centrosomal microtubules from participating directly in the formation of these distal K-fibers.

There are three mechanisms that may contribute to the formation of these distal K-fibers. One possibility is that distal kinetochores capture microtubules that are spontaneously nucleated in the cytoplasm (Rusan et al., 2002). Our observations of several distal K-fiber formation, looping, and capture events showed no single event consistent with this mechanism, and in all cases, the microtubules emerged rapidly from the vicinity of the chromosome (Fig. 1; Fig. S1). Another possibility is that two microtubule bundles nucleated by a centrosome or two unseparated centrosomes may capture each of the two sister kinetochores on a chromosome (syntelic orientation), and the distal K-fiber results from the release of one of these two microtubule fibers. This would be consistent with these distal K-fibers resulting from events correcting syntelic mal-orientations. However, our live cell recordings do not provide any examples of microtubule loops that emerge from monoasters and unravel to form the distal K-fibers, i.e., looping followed by microtubule release. The mechanism that we favor is that these distal K-fibers emerge directly from the kinetochore. Unfortunately, the temporal and spatial resolution of our microscopy does not allow us to determine whether these fibers are directly nucleated by kinetochores (Witt et al., 1980) or emerge from small remnants of previous microtubule attachments. Given that neither NuMA nor γ-tubulin show detectable localization to the minus ends of these growing K-fibers, the identities of the molecules responsible for both this proposed nucleation of kinetochore microtubules and the bundling of kinetochore microtubules into stable K-fibers remain unknown.

Regardless of how distal K-fibers are formed, the fact that they interact with the kinetochore plate in a typical end-on fashion implies that these K-fibers have a polarity such that the plus ends of microtubules are embedded into the kinetochore (Mitchison et al., 1986; Inoue and Salmon, 1995). This means that the free ends of the distal K-fibers corresponded to the minus ends of microtubules. Even though the minus ends of these K-fibers were not associated with centrosomes, the fibers remained stable for many minutes and often exhibited growth (Fig. 1 and Fig. S1). This observed stability of free K-fiber minus ends is not unexpected. Evidence from EM has established that the minus ends of many spindle microtubules, including some kinetochore microtubules, do not terminate at the centrosome (Rieder, 1981; McDonald et al., 1992; Mastronarde et al., 1993). These microtubules are focused at the pole and tethered to the centrosome and its associated astral microtubules by the actions of noncentrosomal structural and motor proteins, such as NuMA, cytoplasmic dynein, and HSET/ncd (Gaglio et al., 1995, 1996, 1997; Merdes et al., 1996; Merdes and Cleveland, 1997; Compton, 1998). Furthermore, minus ends of kinetochore microtubules appear relatively stable even if the centrosome and its astral microtubules are dislocated from the spindle pole (Mitchison and Salmon, 1992; Gordon et al., 2001) or when K-fibers are severed at half length using UV microbeams (Spurck et al., 1990).

The growth of these K-fibers may result from addition of tubulin subunits proximal to the kinetochore. This would be consistent with previous studies where kinetochore-

nucleated microtubule growth has been documented (Mitchison et al., 1986; Geuens et al., 1989). The polewards flux of K-fibers observed in mitotic spindles requires that tubulin subunits be constantly incorporated at microtubule plus ends proximal to the kinetochores (Mitchison, 1989). It is likely that similar mechanisms may contribute to the growth of the distal K-fibers. Further experiments and technological improvements will be needed to clarify the mechanisms of growth and formation of these distal K-fibers.

Incorporation of preformed K-fibers into the spindle. Our second key observation was that over time, the minus ends of preformed K-fibers inevitably exhibited rapid sliding toward the spindle pole and became incorporated into the polar region of the spindle. Specific patterns of the incorporation of the preformed K-fibers depended upon where the minus end of the fiber was located with respect to the pole. Because distal K-fibers were always pointing away from the centrosome in monopolar spindles, their incorporation always involved formation of a transient loop, resulting in syntelic mono-orientation (both K-fibers on one chromosome connected to the same pole). It is noteworthy that this mechanism offers a straightforward explanation for the high frequency of syntelic chromosomes described previously in monastrol-arrested cells (Kapoor et al., 2000).

During spindle bipolarization upon monastrol washout, the geometry of minus-end incorporation was more complex. Those K-fibers that extended away from the separating centrosomes continued to form transient loops, whereas the minus ends of the K-fibers that pointed at the center of the original monopolar spindle exhibited more direct translocations, in both cases toward one of the two separating centrosomes. Importantly, incorporation of preformed K-fibers into the forming spindle was also detected in untreated PtK-αT cells, albeit with lower frequency (Fig. 8). Together, these data reveal that astral arrays of microtubules associated with the centrosomes constantly search for, capture, and incorporate the minus ends of preformed K-fibers.

A question that remains is, how common is the formation and incorporation of K-fibers not connected to centrosomes during normal mitosis? During unperturbed mitosis, such events have not been reported previously. One explanation for this is that these events are difficult to observe. In control mitosis, most chromosomes become amphitelic (properly bioriented) within just a few minutes after NEB. Furthermore, during this time, most chromosomes are in close spatial proximity to one another, and microtubule distribution is too complex for individual K-fibers to be visualized even by modern microscopy. Due to this complexity, most observations on the K-fiber formation were made on individual chromosomes that were incorporated into the spindle at later stages of spindle assembly (for example see Rieder and Alexander, 1990). To circumvent these problems, the formation of K-fibers was studied under special conditions, such as microtubule repolymerization after C-mitosis (Witt et al., 1980; Rieder and Borisy, 1981) or by inhibiting individual components of the spindle using antibody microinjections (Gordon et al., 2001).

Our data reveal that formation and incorporation of K-fibers by the kinetochores is very common in monopolar mitosis. We observed continuous looping over 2-h observation periods with up to 20 events per cell. Further, the frequency of these events did not decrease with time, suggesting that syntelic mal-orientations resulting from these events are not stable and are constantly being corrected. If syntelic chromosomes were stable, then the frequency of looping would gradually decrease as more and more chromosomes would lock in this configuration. We propose that this high frequency of formation and incorporation of K-fibers correlates with the number of chromosomes with kinetochores oriented such that their chromosome bodies sterically shield them from interacting with astral microtubules nucleated from either unseparated centrosome. Therefore, in mono-astral mitoses, the frequent correction of syntelic orientation results in chromosomes with such orientations. In untreated cells, this event is observed at a lower frequency, as only a few chromosomes stochastically orient such that they cannot interact with microtubules from both centrosomes (Fig. 9).

Cassimeris et al. (1994) did not observe any microtubule bundles associated with distal kinetochores in naturally occurring monopolar mitoses in fixed newt lung cells (four serial section EM reconstructions). It is likely that this apparent discrepancy reflects differences between cell types (newt pneumocytes vs. mammalian cells). This may also indicate that the frequency of distal K-fiber formation is somehow increased by monastrol. Consistent with the former proposition, well-developed distal K-fibers have been documented in PtK cells recovering from cold treatment (Rieder and Borisy, 1981). Our observations of distal K-fiber formation in untreated PtK-αT cells (Fig. 8) further suggest that the mechanism of K-fiber formation we observed contributes to normal spindle morphogenesis and is not limited to monastrol-treated cells.

Microtubule minus ends are recruited to centrosomes to determine spindle orientation. Finally, another unexpected phenomenon, conspicuous in our time-lapse recordings, is that during spindle bipolarization upon monastrol washout, the centrosomes transiently detach from the original monopolar spindle and separate independently of the K-fibers, which remain stable and focused. The axis of centrosome separation is unrelated to the original orientation of the focused K-fibers. During separation, the centrosomes remain connected by an array of overlapping interpolar microtubules, forming a spindle-like structure reminiscent of "chromosome-free spindles" (Faruki et al., 2002). Stable K-fibers are gradually recruited by the chromosome-free spindle via capture and incorporation of their minus ends. During this process, the K-fibers bend and reorient to align with the axis of the spindle defined by the separating centrosomes. Thus, the centrosomes appear to be responsible for spindle rotations and for establishing the ultimate orientation of the spindle and the direction of chromosome segregation (O'Connell and Wang, 2000; Khodjakov and Rieder, 2001).

We propose that the major role of the centrosomes during vertebrate mitosis is not to provide dominant sites of microtubule nucleation but rather to establish proper spindle orientation via searching, capturing, and focusing different components of the spindle, i.e., unattached kinetochores, and preformed microtubule bundles, including preformed K-fibers. Formation of K-fibers and bipolar spindles can occur via centrosome-independent mechanisms (for review see Karsenti and Vernos, 2001). However, in the absence of cen-

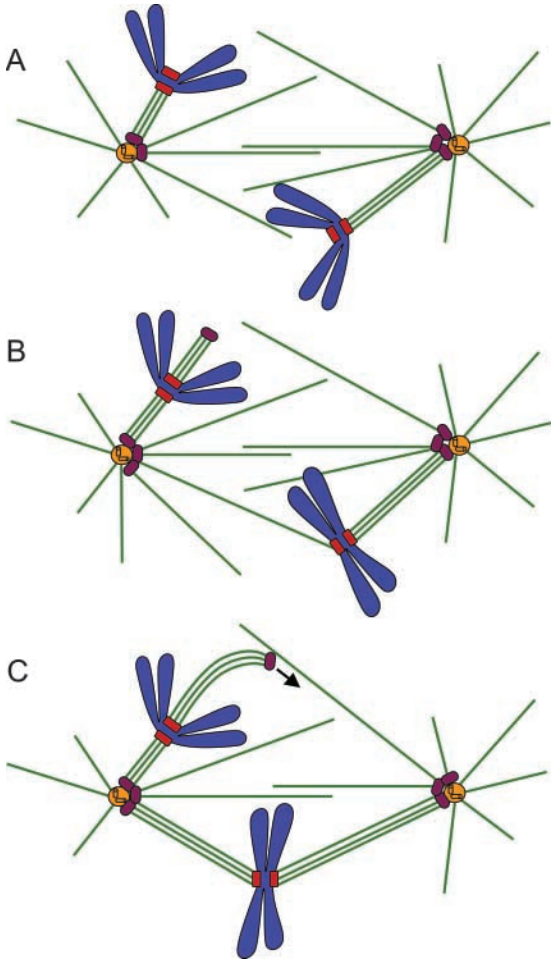

Figure 9. **Two mechanisms contribute to the attachment of chromosomes to spindle poles.** Microtubules (green) grow from centrosomes (yellow, circle) and interact with kinetochores (red) oriented toward the centrosomes. If a sister kinetochore on the mono-oriented chromosome (blue) is oriented toward the distal centrosome (A, right chromosome), its interaction with plus ends of microtubules from the opposite pole is highly probable (B). If the sister kinetochore is shielded from the dense array of microtubules between the two separated centrosomes (A, left chromosome), a K-fiber emanates from the kinetochore and interacts at its minus ends with microtubules connected to centrosomes. NuMA (purple) and associated proteins contribute to the sliding and incorporation of K-fiber minus ends into the spindle (B and C).

trosomes, the spindle is inherently bipolar and incapable of proper orientation, which in turn affects cytokinesis (Khodjakov and Rieder, 2001). By providing astral arrays of microtubules, centrosomes define the number of spindle poles and link the spindle to the cell cortex, providing for proper orientation of the spindle. In this regard, cells of higher plants that are encased in a rigid cell wall, and thus do not need to adjust orientation of the spindle during the course of mitosis, do not possess centrosomes and never form multipolar mitotic spindles (Smirnova and Bajer, 1992).

The search and capture of microtubule plus ends and minus ends during mitosis

The search and capture mechanism proposed by Kirschner and Mitchison (1986) applied only to the capture of plus ends of astral microtubules by kinetochores. Accumulation of new data, including our observations reported here, now allows us to extend this principle onto preformed microtubules (Rusan et al., 2002) and to the minus ends of preformed K-fibers. We propose that the minus-end capture of K-fibers that we have directly observed in vertebrate cells provides a mechanism for a chromosome with such an orientation that its kinetochore cannot encounter dynamic plus ends of microtubules emanating from either centrosomal aster in a bipolar spindle (Fig. 9). A microtubule bundle can grow from the unattached kinetochore and extend beyond the region shielded by the chromosome body. NuMA contributes to the capture of this growing microtubule end by spindle microtubules and, through a motor-dependent activity, facilitates the transport of the K-fiber minus end toward the spindle pole. The polewards transport of NuMA and its interaction with dynein/dynactin have been previously reported and may directly account for this mechanism (Merdes et al., 2000). Together, the plus-end and the minus-end capture of microtubules should account for the attachment of all chromosomes to the spindle during mitosis.

Materials and methods

Cell culture

Stable clones, constitutively expressing α-tubulin/GFP (CLONTECH Laboratories, Inc.), were isolated from the PtK_2 and CV-1 parental cell lines (both purchased from American Type Culture Collection) by G-418 selection and limited-dilution cloning. These clones express growth characteristics very similar to their parental cell lines. LLC-PK cells constitutively expressing α-tubulin/GFP were provided by Patricia Wadsworth (University of Massachusetts, Amherst, MA). PtK-αT cells were maintained in Ham's F12 or DME media supplemented with 10% FBS at 37°C in humidified atmosphere with 5% CO_2. CV-αT and LLC-PK-αT cells were maintained in DME media also supplemented with 10% FBS at 37°C in humidified atmosphere with 5% CO_2.

For time-lapse recordings, cells were transferred onto 24 × 24-mm no. 1.5 coverslips in 50-mm Petri dishes. Approximately 2 h before each experiment, the cultures were mounted in Rose chambers in phenol-free L15 media, supplemented with 10% FBS and 100 μM monastrol. During the widefield microscopy experiments, cells were kept at 34–37°C by a Rose chamber heater (Rieder and Cole, 1998). For confocal microscopy experiments, temperature was controlled using an air curtain (Grego et al., 2001).

For antibody microinjection, CFPAC-1 cells were maintained in Iscove's modified Dulbecco's medium containing 10% FBS at 37°C in a humidified 5% CO_2 atmosphere.

Live cell multimode time-lapse imaging

Near simultaneous widefield GFP fluorescence/DIC time-lapse sequences were collected on a custom-modified Nikon TE-200 microscope equipped with De Senarmont compensation long working distance DIC optics (60XA, 1.4 NA PlanApo lens), a piezo Z-positioning device (Physic Instrumente), and an Orca II cooled CCD camera (Hamamatsu).

Confocal GFP fluorescence time-lapse sequences were acquired on a Carl Zeiss MicroImaging, Inc. Axiovert 200M, a 100×, 1.4 NA, PlanApochromat objective, binning 2 × 2. Confocal sections were imaged with a PerkinElmer Wallac UltraView confocal head with 488-nm excitation filter and argon ion laser (Melles Griot 643R), and an Orca ER cooled CCD camera (Hamamatsu). For DIC image acquisition, a fixed analyzer in the motorized reflector was rotated into position by the software (MetaMorph; Universal Imaging Corp.). Z-projections were performed for fluorescence images using the Carl Zeiss MicroImaging, Inc. Z-motor controlled by the software. In both cases, one DIC image and a stack of five fluorescence images (0.5–1.5-μm steps) were acquired.

Antibody microinjections

CFPAC-1 cells were grown on photo-etched alphanumeric glass coverslips (Bellco Glass Co.) and microinjected as previously described (Gordon et al., 2001). The antibodies used for microinjection were raised against full-

length recombinant NuMA (Gaglio et al., 1995) and the central rod domain of Eg5 (Mountain et al., 1999). IgG was affinity purified from whole serum using protein A–agarose (Roche Molecular Biochemicals), exchanged into microinjection buffer (100 mM KCl, 10 mM KPO_4, pH 7.0) using PD-10 Sephadex G-25 columns (Amersham Biosciences), and injected at concentrations of 5 mg/ml (Eg5) and 20 mg/ml (NuMA).

EM

Cells previously followed in vitro were fixed and prepared for EM according to standard protocols (Khodjakov et al., 1997; Rieder and Cassels, 1999). After flat embedding, they were relocated using phase-contrast microscopy and serially thick sectioned (0.25 μm). The sections were then imaged and photographed in a Carl Zeiss MicroImaging, Inc. 910 microscope operated at 100 kV.

Contours of chromosomes, kinetochores, and adjacent microtubules were traced manually using the Sterecon software package developed at Wadsworth Center (Marko and Leith, 1996). Surface-rendered 3-D models of chromosomes were assembled from the Sterecon tracings in Open Inventor (SGI) software package.

Immunofluorescence microscopy and deconvolution

For immunofluorescence analysis of cells previously followed by time-lapse microscopy, cells were permeabilized with 1% Triton X-100 in PEM buffer (100 mM Pipes, 1 mM EGTA, 5 mM Mg^{2+}, pH 6.9) for 1 min and fixed with 1% glutaraldehyde in PEM. The following antibodies were used: monoclonal anti–γ-tubulin (T6557; Sigma-Aldrich) at 1:300, polyclonal anti-NuMA (Gaglio et al., 1995), monoclonal anti–α-tubulin (Sigma-Aldrich) at 1:300, and polyclonal anti–CENP-E (gift of T. Yen, Fox Chase Cancer Center, Philadelphia, PA). For cells that were immunostained after monastrol washout without time-lapse imaging, cells were fixed and permeabilized for 10 min in 4% formaldehyde solution (100 mM Pipes, 10 mM EGTA, 1mM $MgCl_2$, 0.2% Triton X-100, pH 6.8). In these experiments, γ-tubulin was stained using a rabbit affinity-purified antibody (T5192; Sigma-Aldrich). α-Tubulin was stained with a FITC-conjugated rabbit mAb, DM1A (F2168; Sigma-Aldrich). DNA was stained with Hoechst 33342 (B2261; Sigma-Aldrich). Immunofluorescence images were collected as 3-D volumes on a DeltaVision system (Applied Precision Instruments) and subsequently deconvolved using iterative constrained deconvolution. Seven-pixel-wide line scans were prepared using software tools in Metamorph.

For immunofluorescence analysis of microinjected cells, coverslips were first immersed in microtubule-stabilizing buffer (MTSB; 4 M glycerol, 100 mM Pipes, pH 6.8, 1 mM EGTA, 5 mM $MgCl_2$) for 1 min, followed by a 2-min extraction in MTSB/0.5% Triton X-100. Cells were then rinsed in MTSB for 2 min and fixed in 1% glutaraldehyde. The glutaraldehyde was quenched with two 10-min rinses in 0.5 mg/ml $NaBH_4$, and the cells were rinsed in TBS (10 mM Tris, pH 7.5, 150 mM NaCl) containing 1% BSA (TBS-BSA) for 5 min. α-Tubulin was stained for using the mouse monoclonal antibody DM1α (Sigma-Aldrich), and centrosomes were detected with a human α-centrosome antibody provided by J.B. Rattner (University of Calgary, Calgary, Alberta, Canada). DNA was stained with DAPI (Sigma-Aldrich).

Online supplemental material

Time-lapse movies (Videos 1–4) and a supplementary figure (Fig. S1) are available at http://www.jcb.org/cgi/content/full/jcb.200208143/DC1.

We acknowledge use of Wadsworth Center's Light and Electron Microscopy core facilities and Alison North and the Rockefeller University BioImaging Facility.

This work was supported by National Institutes of Health grants GM59363 (A. Khodjakov), GM51542 (D.A. Compton), and GM65933 (T.M. Kapoor).

Submitted: 23 August 2002
Revised: 28 January 2003
Accepted: 28 January 2003

References

Bajer, A.S. 1982. Functional autonomy of monopolar spindle and evidence for oscillatory movement in mitosis. *J. Cell Biol.* 93:33–48.

Bonaccorsi, S., M.G. Giansanti, and M. Gatti. 1998. Spindle self-organization and cytokinesis during male meiosis in asterless mutants of *Drosophila melanogaster*. *J. Cell Biol.* 142:751–761.

Cassimeris, L., C.L. Rieder, and E.D. Salmon. 1994. Microtubule assembly and kinetochore directional instability in vertebrate monopolar spindles: implications for the mechanism of chromosome congression. *J. Cell Sci.* 107(Pt. 1): 285–297.

Compton, D.A. 1998. Focusing on spindle poles. *J. Cell Sci.* 111(Pt. 11):1477–1481.

Faruki, S., R.W. Cole, and C.L. Rieder. 2002. Separating centrosomes interact in the absence of associated chromosomes during mitosis in cultured vertebrate cells. *Cell Motil. Cytoskeleton.* 52:107–121.

Gaglio, T., A. Saredi, and D.A. Compton. 1995. NuMA is required for the organization of microtubules into aster-like mitotic arrays. *J. Cell Biol.* 131:693–708.

Gaglio, T., A. Saredi, J.B. Bingham, M.J. Hasbani, S.R. Gill, T.A. Schroer, and D.A. Compton. 1996. Opposing motor activities are required for the organization of the mammalian mitotic spindle pole. *J. Cell Biol.* 135:399–414.

Gaglio, T., M.A. Dionne, and D.A. Compton. 1997. Mitotic spindle poles are organized by structural and motor proteins in addition to centrosomes. *J. Cell Biol.* 138:1055–1066.

Gordon, M.B., L. Howard, and D.A. Compton. 2001. Chromosome movement in mitosis requires microtubule anchorage at spindle poles. *J. Cell Biol.* 152: 425–434.

Grego, S., V. Cantillana, and E.D. Salmon. 2001. Microtubule treadmilling in vitro investigated by fluorescence speckle and confocal microscopy. *Biophys. J.* 81:66–78.

Geuens, G., A.M. Hill, N. Levilliers, A. Adoutte, and M. DeBrabander. 1989. Microtubule dynamics investigated by microinjection of *Paramecium* axonemal tubulin: lack of nucleation but proximal assembly of microtubules at the kinetochore during prometaphase. *J. Cell Biol.* 108:939–953.

Gruss, O.J., M. Wittmann, H. Yokoyama, R. Pepperkok, T. Kufer, H. Sillje, E. Karsenti, I.W. Mattaj, and I. Vernos. 2002. Chromosome-induced microtubule assembly mediated by TPX2 is required for spindle formation in HeLa cells. *Nat. Cell Biol.* 4:871–879.

Heald, R., R. Tournebize, T. Blank, R. Sandaltzopoulos, P. Becker, A. Hyman, and E. Karsenti. 1996. Self-organization of microtubules into bipolar spindles around artificial chromosomes in *Xenopus* egg extracts. *Nature.* 382: 420–425.

Inoue, S., and E.D. Salmon. 1995. Force generation by microtubule assembly/disassembly in mitosis and related movements. *Mol. Biol. Cell.* 6:1619–1640.

Karsenti, E., and I. Vernos. 2001. The mitotic spindle: a self-made machine. *Science.* 294:543–547.

Kapoor, T.M., T.U. Mayer, M.L. Coughlin, and T.J. Mitchison. 2000. Probing spindle assembly mechanisms with monastrol, a small molecule inhibitor of the mitotic kinesin, Eg5. *J. Cell Biol.* 150:975–988.

Khodjakov, A., and C.L. Rieder. 1999. The sudden recruitment of γ-tubulin to the centrosome at the onset of mitosis and its dynamic exchange throughout the cell cycle do not require microtubules. *J. Cell Biol.* 146:585–596.

Khodjakov, A., and C.L. Rieder. 2001. Centrosomes enhance the fidelity of cytokinesis in vertebrates and are required for cell cycle progression. *J. Cell Biol.* 153:237–242.

Khodjakov, A., R.W. Cole, B.F. McEwen, K.F. Buttle, and C.L. Rieder. 1997. Chromosome fragments possessing only one kinetochore can congress to the spindle equator. *J. Cell Biol.* 136:229–240.

Khodjakov, A., R.W. Cole, B.R. Oakley, and C.L. Rieder. 2000. Centrosome-independent mitotic spindle formation in vertebrates. *Curr. Biol.* 10:59–67.

Kirschner, M., and T. Mitchison. 1986. Beyond self-assembly: from microtubules to morphogenesis. *Cell.* 45:329–342.

Kufer, T.A., H.H. Sillje, R. Korner, O.J. Gruss, P. Meraldi, and E.A. Nigg. 2002. Human TPX2 is required for targeting Aurora-A kinase to the spindle. *J. Cell Biol.* 158:617–623.

Marko, M., and A. Leith. 1996. Stereocon–three-dimensional reconstructions from stereoscopic contouring. *J. Struct. Biol.* 116:93–98.

Mastronarde, D.N., K.L. McDonald, R. Ding, and J.R. McIntosh. 1993. Interpolar spindle microtubules in PTK cells. *J. Cell Biol.* 123:1475–1489.

Mayer, T.U., T.M. Kapoor, S.J. Haggarty, R.W. King, S.L. Schreiber, and T.J. Mitchison. 1999. Small molecule inhibitor of mitotic spindle bipolarity identified in a phenotype-based screen. *Science.* 286:971–974.

McDonald, K.L., E.T. O'Toole, D.N. Mastronarde, and J.R. McIntosh. 1992. Kinetochore microtubules in PTK cells. *J. Cell Biol.* 118:369–383.

Megraw, T.L., L.R. Kao, and T.C. Kaufman. 2001. Zygotic development without functional mitotic centrosomes. *Curr. Biol.* 11:116–120.

Merdes, A., and D.W. Cleveland. 1997. Pathways of spindle pole formation: different mechanisms; conserved components. *J. Cell Biol.* 138:953–956.

Merdes, A., K. Ramyar, J.D. Vechio, and D.W. Cleveland. 1996. A complex of NuMA and cytoplasmic dynein is essential for mitotic spindle assembly.

Cell. 87:447–458.

Merdes, A., R. Heald, K. Samejima, W.C. Earnshaw, and D.W. Cleveland. 2000. Formation of spindle poles by dynein/dynactin-dependent transport of NuMA. *J. Cell Biol.* 149:851–862.

Mitchison, T., L. Evans, E. Schulze, and M. Kirschner. 1986. Sites of microtubule assembly and disassembly in the mitotic spindle. *Cell.* 45:515–527.

Mitchison, T.J. 1989. Polewards microtubule flux in the mitotic spindle: evidence from photoactivation of fluorescence. *J. Cell Biol.* 109:637–652.

Mitchison, T.J., and E.D. Salmon. 1992. Poleward kinetochore fiber movement occurs during both metaphase and anaphase-A in newt lung cell mitosis. *J. Cell Biol.* 119:569–582.

Mountain, V., C. Simerly, L. Howard, A. Ando, G. Schatten, and D.A. Compton. 1999. The kinesin-related protein, HSET, opposes the activity of Eg5 and cross-links microtubules in the mammalian mitotic spindle. *J. Cell Biol.* 147: 351–366.

O'Connell, C.B., and Y.L. Wang. 2000. Mammalian spindle orientation and position respond to changes in cell shape in a dynein-dependent fashion. *Mol. Biol. Cell.* 11:1765–1774.

Rieder, C.L. 1981. The structure of the cold-stable kinetochore fiber in metaphase PtK1 cells. *Chromosoma.* 84:145–158.

Rieder, C.L., and S.P. Alexander. 1990. Kinetochores are transported poleward along a single astral microtubule during chromosome attachment to the spindle in newt lung cells. *J. Cell Biol.* 110:81–95.

Rieder, C.L., and G.G. Borisy. 1981. The attachment of kinetochores to the prometaphase spindle in PtK1 cells. Recovery from low temperature treatment. *Chromosoma.* 82:693–716.

Rieder, C.L., and G. Cassels. 1999. Correlative light and electron microscopy of mitotic cells in monolayer cultures. *Methods Cell Biol.* 61:297–315.

Rieder, C.L., and R.W. Cole. 1998. Perfusion chambers for high-resolution video light microscopic studies of vertebrate cell monolayers: some considerations and a design. *Methods Cell Biol.* 56:253–275.

Rieder, C.L., and R. Hard. 1990. Newt lung epithelial cells: cultivation, use, and advantages for biomedical research. *Int. Rev. Cytol.* 122:153–220.

Rieder, C.L., and E.D. Salmon. 1998. The vertebrate cell kinetochore and its roles during mitosis. *Trends Cell Biol.* 8:310–318.

Roos, U.P. 1976. Light and electron microscopy of rat kangaroo cells in mitosis. III. Patterns of chromosome behavior during prometaphase. *Chromosoma.* 54:363–385.

Rusan, N.M., U.S. Tulu, C. Fagerstrom, and P. Wadsworth. 2002. Reorganization of the microtubule array in prophase/prometaphase requires cytoplasmic dynein-dependent microtubule transport. *J. Cell Biol.* 158:997–1003.

Smirnova, E.A., and A.S. Bajer. 1992. Spindle poles in higher plant mitosis. *Cell Motil. Cytoskeleton.* 23:1–7.

Spurck, T.P., O.G. Stonington, J.A. Snyder, J.D. Pickett-Heaps, A. Bajer, and J. Mole-Bajer. 1990. UV microbeam irradiations of the mitotic spindle. II. Spindle fiber dynamics and force production. *J. Cell Biol.* 111:1505–1518.

Walczak, C.E., I. Vernos, T.J. Mitchison, E. Karsenti, and R. Heald. 1998. A model for the proposed roles of different microtubule-based motor proteins in establishing spindle bipolarity. *Curr. Biol.* 8:903–913.

Witt, P.L., H. Ris, and G.G. Borisy. 1980. Origin of kinetochore microtubules in Chinese hamster ovary cells. *Chromosoma.* 81:483–505.